BIOLOGY OF REPRODUCTION 43, 485–491 (1990)

Dense Fibers Protect Mammalian Sperm against Damage[1]

JAY M. BALTZ,[2] P. ONEEKA WILLIAMS, and RICHARD A. CONE

The Jenkins Department of Biophysics, The Johns Hopkins University, Baltimore, MD 21218

ABSTRACT

The relative tensile strengths of the sperm of seven mammalian species and sea urchins have been measured by determining the minimum shear necessary to kill them (assayed by lack of motility) when they are suspended in a viscous fluid. In general, long sperm are killed by smaller shears than short sperm. However, the longer sperm are not as fragile as would be expected from theoretical predictions. Their additional tensile strength correlates well with the size of their dense fibers; a theory that includes the dense fiber contributions accurately predicts the sperm tensile strength for most of the species in which this has been measured. This added strength may be necessary to protect sperm from shear forces encountered during epididymal transport and especially during ejaculation, as these forces are strong enough to kill long sperm if they are not strengthened.

INTRODUCTION

Cardullo and Cone [1], during the course of metabolic measurements, observed that rat sperm are more susceptible to damage than are bull sperm when the fluid in which they are suspended is stirred. We wondered whether this greater fragility of rat sperm was due to their greater length: rat sperm are about 189 μm long, whereas bull sperm are only about 54 μm long. If, indeed, larger sperm are more fragile, there would be many mammalian species with fragile sperm; mammalian sperm span a wide range of lengths: published values range from 33 μm for the hippopotamus (*Hippopotamus amphibius*) to 356 μm for the honey possum (*Tarsipes rostratus*) [2, 3].

Sperm fragility could pose a problem for animals with larger sperm, since sperm experience fluid shear not only during artificial situations such as stirring in vitro, but also during in vivo epididymal transport and ejaculation.

We have developed a method to quantify sperm fragility by subjecting them to defined shears in a fluid of known viscosity. Using this method with sperm from a number of species, we can test the hypothesis that long sperm are generally more fragile than short sperm. Also, the presence of any mechanism that strengthens sperm can be detected by comparing the theoretically predicted tensile strength with that measured.

MATERIALS AND METHODS

Chemicals and Solutions

Chemicals were purchased from Baker Chemicals (Phillipsburg, NJ). Methylcellulose (2% solution = 4 000 cP) was from Sigma (St. Louis, MO).

The medium for epididymal sperm was PSS [1], which contains 138 mM NaCl, 3.5 mM KCl, 0.18 mM $CaCl_2$, 0.18 mM $MgCl_2$, 12 mM Na_2HPO_4, and 2.2 mM NaH_2PO_4 (pH 7.4, approximately 285 mOsM). A modified version, designated PSSD, with 0.9 mM $CaCl_2$ and $MgCl_2$, was used with ejaculated human sperm [4]. Artificial sea water (ASW; pH 8.0, approximately 870 mOsM) was used with sea urchin sperm.

Animals and Sperm Collection

Mice (*Mus musculus*), golden hamsters (*Mesocricetus auratus*), chinese hamsters (*Cricetulus griseus*), guinea pigs (*Cavia porcellus*), and rats (*Rattus norvegicus*) were purchased from Charles River Breeding Labs., Wilmington, MA). They were anesthetized with phenobarbital, killed either by cervical dislocation or by an overdose of chloroform, and the epididymides were excised. Bull (*Bos taurus*) epididymides were obtained from Schmidt's, Inc. (Baltimore, MD). Epididymal sperm were collected by puncturing the cauda epididymidis; the extruded epididymal contents were diluted with approximately 100 μl PSS and centrifuged gently. Rat sperm did not tolerate centrifugation well and were simply diluted into PSS. Ejaculated human sperm were collected by allowing them to swim up into a layer of 1 ml PSSD overlying 0.5 ml semen. Sea urchin (*Lytechinus variegatus* and *Strongylocentrotus purpuratus*) sperm were collected after intracoelomic injection of 0.5 M KCl and were diluted directly into ASW. All sperm concentrations were adjusted to 10^8/ml with PSSD (human), ASW (sea urchin), or PSS (all others).

Measuring Sperm Fragility

Forces on a body subject to shear. The usual means of envisioning the production of constant, one-dimensional shear is a system of two parallel plates separated by a distance y_o, with a fluid between them; one plate is at rest while the other moves at a constant velocity v_o (Fig.1). The fluid velocity then varies linearly from 0 to v_o, and the shear rate is v_o/y_o. For an excellent discussion, the reader is directed to Feynmann et al. [5].

Accepted May 7, 1990.
Received January 10, 1990.
[1]Supported by NIH HD16800.
[2]Correspondence at current address: Dr. Jay M. Baltz, Laboratory of Human Reproduction and Reproductive Biology, Harvard Medical School, 45 Shattuck Street, Boston, MA 02115.

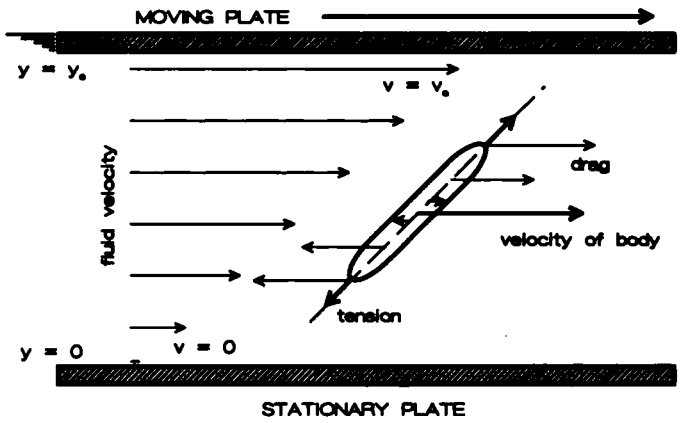

FIG. 1. Constant shear produced by relative motion of parallel plates. The velocity of the fluid (moving to the right) increases linearly with distance from the bottom plate (at $y = 0$), which is stationary, to the top plate (at $y = y_o$), whose velocity is v_o. The shear rate is constant, and has the value v_o/y_o. The arbitrary body shown in this flow moves to the right, but experiences varying velocities along its length. The top is dragged to the right and the bottom to the left, resulting in tension along the axis of the body.

The viscous drag on a long, thin body in a slow, constant flow is roughly proportional to the longest dimension of the body, to the velocity of the flow, and to the viscosity of the fluid. However, it varies only very slowly with the width of the body, which can be neglected. In a constant flow, the object will simply move with the same velocity as the fluid. However, in fluid subjected to a constant shear, a body will experience a gradient of velocities along its length (Fig. 1) and will move at approximately the average of these velocities. Those parts of the body extending into slower flows will be dragged back, while those parts that extend into faster flows will be dragged forward. Therefore, the object will be under tension (and will also rotate).

How does the tension depend on the length? We will assume a long, thin body with a constant cross section, which is approximately valid for a sperm flagellum. The tension, for example at the center, is the sum of all the drag components on (infinitesimal) segments above the center pulling up, plus those for segments below the center pulling down. The drag on each segment is proportional to the fluid velocity relative to the segment, and the viscosity of the fluid.

For a constant shear, the velocity at any segment relative to that at the center is proportional to the product of the shear rate and the distance from the center. Therefore, the drag on each segment is proportional to the viscosity, the shear rate, and the distance from the center. The total tension is obtained by integrating over the length. Thus, the tension is proportional to the viscosity, the shear rate, and the length squared:

$$F_T = CK\eta L^2 \quad (1)$$

where F_T is tension, C is a dimensionless constant, K is the shear rate, η is the viscosity, and L is the length. Rotation and orientation with respect to the flow have been ignored here because almost all bodies in a one-dimensional shear will "tumble" and not assume any preferred orientation [6, 7]; they will thus experience the maximum tension for at least some period during each "tumble."

We subjected sperm to tension of this type by shearing the fluid in which they were suspended. If all sperm have the same intrinsic strength, they will act analogously to chains of different lengths, which will break under the tension needed to break one link, regardless of length. This would be the case if the axonemes, which are highly conserved among all species, were the major determinant of tensile strength.

To reach a given tension on a sperm, a shear rate must be imposed that is inversely proportional to its length squared, as can be seen from Equation 1. Therefore, if all sperm have the same intrinsic strength and are all damaged by the same tension, the minimum shear rate that damages any sperm will also be proportional to the inverse of its length squared:

$$K_L = T_S/(C\eta L^2) \quad (2)$$

where K_L is the lethal shear rate, i.e. the minimum shear rate that causes lethal damage, and T_S is a force equal to the tensile strength of a sperm (which we are assuming to be constant independent of length).

Apparatus for shearing sperm. It is not practical to use parallel plates in a shearing device. Instead, we used an apparatus in which a cone rotates with its point against a plate (Fig. 2). The velocity increases linearly with distance from the point of the cone, but the separation between the cone and plate also increases linearly, yielding constant shear

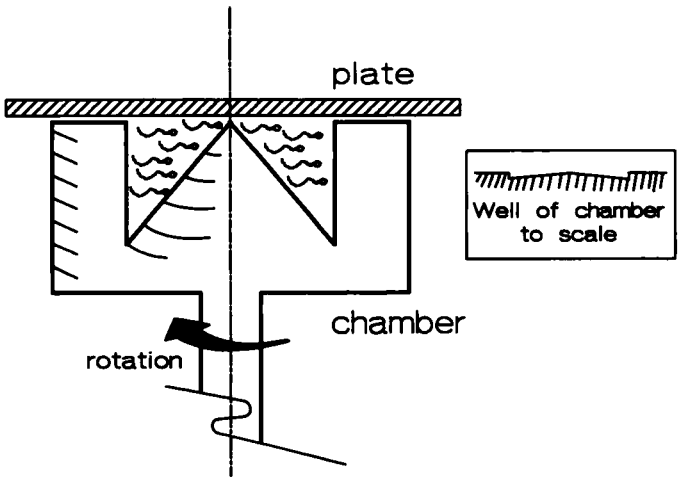

FIG. 2. The "cone and plate" shear apparatus. The radius of the well of the chamber was 0.5 cm, and its depth at the edge was 0.0475 cm, yielding a volume of approximately 25 μl. The well was machined into a stainless steel cylinder (radius = 1 cm, height = 1 cm) with a shaft at the bottom for mounting. The well, which is shown with a greatly exaggerated vertical scale for clarity, is shown to actual scale in the inset at right. It is sufficiently wide and shallow that edge effects are negligible. Glass microscope slides were used as the plates. See *text* for further description.

(velocity/distance) throughout most of the fluid between the cone and plate.

The apparatus, as shown in Figure 2, was made by the Johns Hopkins University Machine Shop. A stainless steel rotating chamber with a conical floor, mounted on a variable-speed motor (Cole-Parmer, Chicago, IL) controlled by a timer (Spiratone model 30, Flushing NY), was held against a stationary glass plate (microscope slide). Shear rates to 5 500 s^{-1} were possible.

Fluid used for sperm shearing. The flow of water is quite turbulent at the velocities obtained with this apparatus, and the viscosity of water is too low to produce the necessary forces at the shear rates possible in this apparatus. These problems were avoided by adding methylcellulose (MC) to the basic media to increase their viscosity. However, since MC solutions are nonnewtonian in that the viscosity is a function of the shear rate, we constructed a simple "high-shear" viscometer to measure the shear-dependent viscosity of MC solutions.

The apparent viscosity of a sample can be measured by forcing it through a tube and using Poiseuille's equation:

$$\eta = P \pi R^4/(8F \ell) \quad (3)$$

where F is the rate of flow, ℓ is the length of the tube, P is the pressure driving the fluid through the tube, and R is the radius of the tube. This equation is strictly true only for newtonian fluids. However, since the apparent viscosity of these MC solutions is only a weak function of shear over the shear range we used with sperm (>1 000 s^{-1}), these viscosity measurements yield a good approximation of the true viscosity. In our viscometer, the sample was loaded into a clear plastic chamber marked in 0.05-ml increments. Known pressure was applied to one end of this chamber by a 60-ml plastic syringe in which 60 ml air was compressed to various volumes, forcing the fluid through the measuring tube (26 g, 0.5-inch hypodermic needle with inner radius = 0.013 cm) at the other end of the sample chamber. The flow rate was measured by timing how long 0.05 ml of the sample took to pass through the tube. The maximum shear rate was determined from the flow rate and needle radius, and was given by $4F/\pi R^3$ assuming a parabolic flow profile (rates of up to about 10 000 s^{-1} could be obtained). The accuracy of the viscometer was verified to be ±15% using the newtonian fluids glycerol and Dow 200 silicon.

Two percent MC in PSS (or PSSD) was used for mammalian sperm. However, because of the greater salt concentration, we had to use 2.5% MC in ASW to obtain comparable apparent viscosities. Figure 3 shows the apparent viscosity vs. shear rate for both solutions. The measured viscosity at each shear rate was used in Equations 1 and 2.

Lethal shear stress. The product of the viscosity and the shear rate that appears in Equation 1 is called the shear stress and has the units of force per unit area. Thus, Equation 1 can be rewritten as:

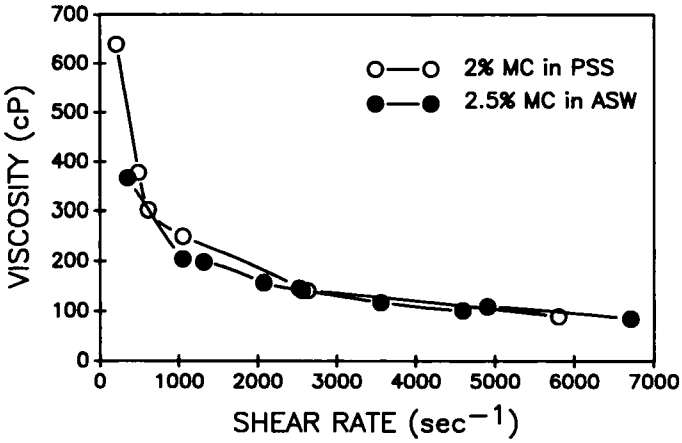

FIG. 3. Shear-dependent viscosity of methylcellulose (MC) solutions. MC thins with increasing shear. A high-shear viscometer was used to determine the viscosity of the test solutions (see *text*) as a function of the imposed shear rate.

$$F_T = CSL^2 \quad (4)$$

where S is the shear stress, calculated from the product of the shear in the chamber and the viscosity measured for that shear. Conveniently, it combines both of the measured parameters, K and η. Equation 2 becomes:

$$S_L = T_S/CL^2 \quad (5)$$

where S_L is the lethal shear stress (where the number of motile sperm after shearing fell to one-half of the control level).

We have equated immotile sperm with dead sperm throughout this work, since Cardullo and Cone [1] found that sperm rendered immotile by shearing ceased consuming oxygen and, presumably, were dead.

Experimental Procedure

Fifty microliters of sperm solution was mixed, by gentle stirring, with 100 μl of 1.5-strength MC stock in one well of a 96-well microtiter plate. This mixture was then drawn up, by mouth suction, in a 50-μl wiretrol pipette and about 30 μl was placed in the chamber. The remainder was kept in the pipette to serve as the control sample. The glass slide was placed over the chamber and held down firmly. The motor was then triggered and shearing of the sample lasted 1.5 s (regulated by the timer). The chamber reached full speed in less than 0.2 s and stopped in less than 0.5 s (as determined by strobe measurements). After shearing, the sample was placed on a microscope slide. The same volume of the control sample was placed elsewhere on the same slide. About one-half the sample volume of medium was added to each drop (to decrease the viscosity and allow vigorous motility) and slowly mixed in. A coverslip was then placed on each drop, and the sperm were observed on an Olympus BH2 microscope with Nomarski interference contrast optics using a 20× objective. The motility rel-

ative to the control drop was scored on a scale of 0 (immotile) to 4 (motility indistinguishable from that of the control). We found that the precision of this scale was the greatest that yielded reproducible results. This procedure was then repeated for a number of different shear rates, each time using new aliquots of the sperm sample. A curve was constructed for each species giving the motility as a function of shear stress. Since the sperm of the two sea urchin species were virtually identical, the sea urchin data were pooled.

RESULTS AND DISCUSSION

Lethal Shears for Various Species

The effect of shear stress on sperm motility was determined for mice, bulls, hamsters, chinese hamsters, guinea pigs, rats, humans, and one nonmammalian species—sea urchins (Fig. 4). The lethal shear stress for each species was taken to be that shear stress where the curve fitted to the experimental data passed through a motility score of 2, where, on average, half the motile sperm in the sample were killed (judged relative to the control). The lethal shear stresses were 4 200 dynes/cm^2 for bull sperm, 4 500 for human, 4 300 for guinea pig, 2 500 for mouse, 2 200 for hamster, 2 600 for rat, 2 000 for chinese hamster, and 3 600 for sea urchin.

After exposure to shear stresses at or somewhat above the lethal shear stress, sperm appeared to be normal except for lack of motility. It is probable that stretching during shearing disrupted internal flagellar structures and/or the membrane, rendering the sperm immotile, but that this was not visible at the light microscope level. At higher shears, tails broke or separated from heads.

Lethal Shear vs. Length

The lethal shear stresses found for the various species are shown in Figure 5 as a function of the length of the sperm. The lengths of the sperm were 54 μm (bull), 58 μm (human), 107 μm (guinea pig), 123 μm (mouse), 187 μm (hamster), 189 μm (rat), 258 μm (chinese hamster) (lengths from Cummins and Woodall, [3]; average was used when several given), and 45 μm (sea urchins, Gray, [8]; Rikmenspoel, [9]; Brokaw and Gibbons, [10]. As expected, the longer sperm were indeed more fragile than the shorter sperm. However, the lethal shear stress did not vary inversely with the length squared (Equation 5), as clearly shown in Figure 5. Indeed, the longer sperm were much stronger relative to the shorter sperm than expected; rather than falling by 30-fold from the shortest to the longest sperm, as required for a length-squared dependence, the lethal shear stress fell by only a factor of two. This difference revealed that the longest sperm had appoximately 15 times greater intrinsic strength than the smallest sperm. Therefore, the axoneme, which is relatively constant in all species, could not be the primary determinant of the tensile strength of all these sperm. Rather, some structures exist in sperm that confer increasing tensile strength with increasing length.

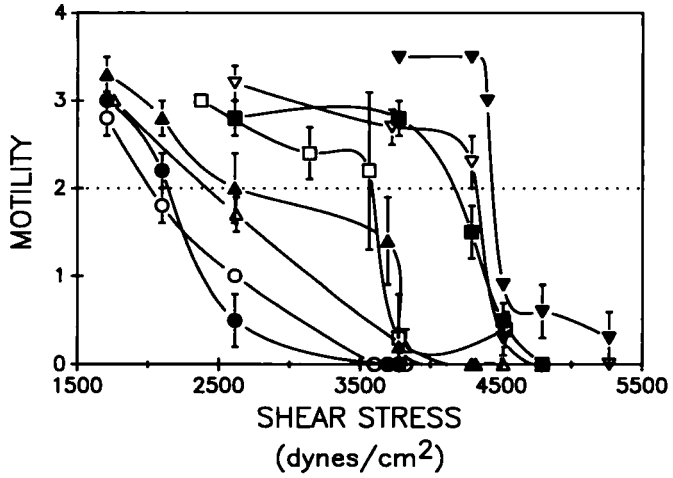

FIG. 4. Motility of sperm of various species after being sheared. Sperm motility is shown as a function of the shear stress to which sperm were subjected. Each point represents at least 4 measurements, with 4–10 animals of each species used. Error bars give standard error of the mean; a lack of error bars means that the error is smaller than the symbol. The curves were fit using a cubic spline (Sigmaplot, Jandel Scientific, Sausalito, CA). The lethal shear stress was taken to be the shear stress that caused motility to fall to a motility score of 2 (about one-half the control level), indicated by the dotted line. For clarity of presentation, only data from the region around this point are shown for each species.

The species are indicated as follows: ○ chinese hamster, ● hamster, △ mouse, ▲ rat, □ sea urchin (data for both species pooled), ■ bull, ▽ guinea pig, and ▼ human.

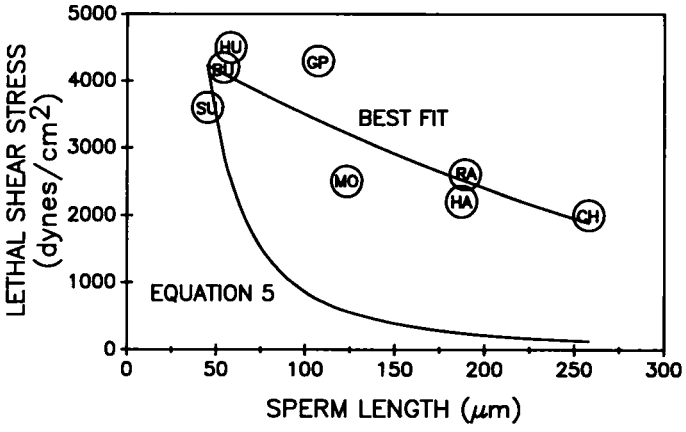

FIG. 5. Lethal shear stress vs. length of sperm. The measured lethal shear stresses for the sperm of seven mammalian species and the sea urchin are shown as a function of the length of the sperm, along with the best-fit curve to these points (a second order polynomial was fit by least-squares regression, $R^2 = 0.71$). The dependence of lethal shear on sperm length predicted by Equation 5, namely that the tensile strength of the sperm is inversely proportional to the length squared, is also plotted. It was normalized to the best-fit curve at $L = 45$ μm, the shortest sperm type in our sample. The symbols indicate the animal: sea urchin (SU), bull (BU), human (HU), guinea pig (GP), mouse (MO), hamster (HA), rat (RA), and chinese hamster (CH).

What Strengthens Longer Sperm?

The obvious candidates for structures that could contribute to the tensile strength of sperm are the nine dense outer fibers that surround the axoneme in mammalian sperm. They are found in every species of mammalian sperm, but their function is unknown. It has been demonstrated, however, that the added stiffness that thick, dense fibers confer affects the pattern of motility [11].

To test the hypothesis that the dense outer fibers are responsible for the increased tensile strength of the longer sperm, we assumed that the tensile strength of a sperm is the sum of a constant component reflecting the axoneme and other conserved structures (T_{ax}), and a component arising from the dense fibers (T_{df}):

$$T_S = T_{ax} + T_{df} \quad (6)$$

Furthermore, we assumed that the tensile strength of the dense fibers is proportional to their cross-sectional area, yielding:

$$T_S = T_{ax} + DA_{df} \quad (7)$$

where A_{df} is the total cross-sectional area of the dense fibers and D is a constant. Substituting for the formerly constant tensile strength (T_S) in Equation 5 yields:

$$S_L = (T_{ax} + DA_{df})/CL^2 \quad (8)$$

To find the lethal shear stresses predicted by Equation 8, we must find the cross-sectional areas of the dense fibers of each of these species.

Each fiber becomes progressively thinner as it extends down the length of the flagellum towards the distal end, and each terminates a different distance from the head [12, 13]. To compare fiber areas between species, the areas must be determined at corresponding positions on the flagellum. We compared the cross-sectional areas of the fibers in the easily identified midpiece region of each of the mammalian species whose sperm were used in the shear experiments. We further assumed that the cross-sectional areas throughout the length of the flagellum are proportional to those in the midpiece. Sea urchins have no dense fibers and thus, for them, A_{df} is zero. However, their axoneme is virtually indistinguishable from those of mammals, so the axonemal component of tensile strength should be identical to that of mammalian sperm. Figure 6 shows drawings of cross sections through the midpiece indicating the relative cross-sectional areas of the dense fibers of the species we used. The measured total areas of the fibers are shown under each cross section (given in μm^2; see figure legend).

How well does this new model in which the tensile strength of sperm is the sum of the tensile strength due to the axoneme plus that due to the dense fibers predict the strength of the sperm? This was determined by using Equation 8 with the measured cross-sectional areas of the dense fibers to predict the lethal shear stresses, and then comparing these to the measured values. We rearranged Equation 8 as:

$$S_L L^2 = (T_{ax}/C) + (D/C)A_{df} \quad (9)$$

which indicates a linear relationship between $S_L L^2$ and A_{df} if the dense fibers are the source of the additional tensile strength. A linear least-squares regression confirmed that this was a linear relationship for these data. The data for bull sperm were an exception, however, lying well above those for the other species. That is, bull sperm were much more fragile than was predicted by the size of their dense fibers. For this reason, we did not include the data for bull in the following analysis, but they will be discussed below.

Without the data for bull sperm, the linear relationship predicted by Equation 9 was very tight ($R^2 = 0.91$). The values of the slope and intercept provided values for the constant coefficients, D/C and T_{ax}/C, and Equation 9 becomes:

$$S_L = (0.07 + 5.3 \times 10^8 A_{df})/L^2 \quad (10)$$

S_L is in dynes/cm^2, A_{df} is in cm^2, and L is in cm. Figure 7 shows the values of the lethal shear stress predicted by Equation 10 (diamonds), along with those measured experimentally (circles). The mean of the absolute values of the errors between the measured and predicted values was 17%, which is within experimental error. This good agreement indicated that the tensile strength of these mammalian sperm could be determined by the constant strength of the axoneme plus the variable added strength of the dense fibers.

A comparison of the terms in Equation 10 reveals that most of the tensile strength in the mammalian species arose from the dense fibers. Furthermore, this proportion generally increased with increasing sperm length; dense fibers accounted for only 60% of the tensile strength of human sperm, but 94% of the tensile strength of chinese hamster sperm.

Sea urchin sperm had the tensile strength predicted for a mammalian sperm lacking dense fibers. All the dense fiber-containing mammalian sperm were found to have greater intrinsic tensile strengths than sea urchin sperm.

Why Do Bull and Guinea Pig Sperm Exhibit Anamalous Tensile Strengths?

The prediction of guinea pig sperm tensile strength was a bit worse than most, with the measured tensile strength falling about 50% below that which we predicted. The prediction for bull sperm was much worse, as mentioned above, with the measured tensile strength falling 4-fold below the predicted strength. Yet, even for bull sperm, the prediction was much better than that afforded by Equation 5, where the errors in prediction were as much as 15-fold.

The poor prediction of the strength of bull sperm (and to a much lesser extent, guinea pig sperm) may have been

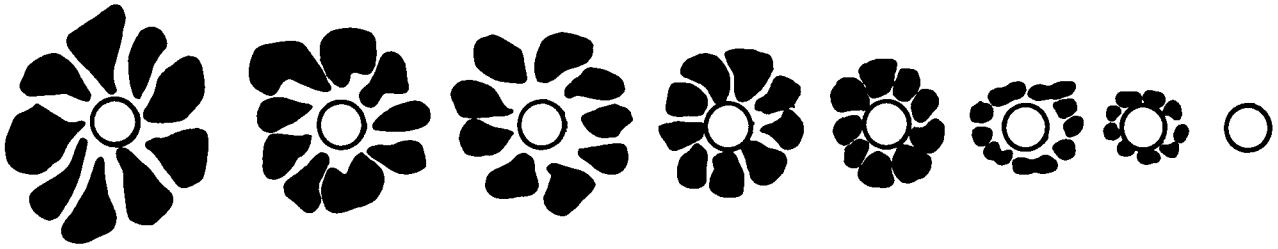

FIG. 6. Cross-sectional area of dense outer fibers of sperm. The dense fibers as they appear in the midpiece regions of the species we used are shown. The circles at the center indicate the size of the axoneme. The sea urchin is represented by the circle alone, since it possesses no accessory fibers. The areas (in μm^2) shown below each species were measured by cutting out the images of the nine fibers traced from micrographs in the original sources cited below, weighing them, and correcting for differences in the scales of the micrographs. These drawings are adapted from the micrographs used, adjusted so that the scale is the same for all species. The original micrographs were found in the following sources: human, Serres et al. [13]; mouse and rat, Phillips [11]; bull, Lindemann and Gibbons [23]; hamster, Yanagimachi et al., [24]; chinese hamster and guinea pig, Fawcett [14]. Several of these areas were checked using micrographs from other sources; the areas found were essentially identical (data not shown).

due to our assumption that the dense fibers were everywhere proportional to their sizes in the midpiece. The anomalous weakness of bull and guinea pig sperm, given the large size of their dense fibers in the midpiece, could be explained if the fibers extend over a smaller fraction of the length of the flagellum or taper more sharply than in other species. Slightly short or more tapered fibers could account for the 50% error for guinea pig sperm; indeed, indications that the size of dense fibers in the midpiece does not necessarily predict the size further down the flagellum are seen when guinea pig sperm flagellar sections are compared to those of the chinese hamster [14]; guinea pig dense fibers seem to be smaller in the principal piece

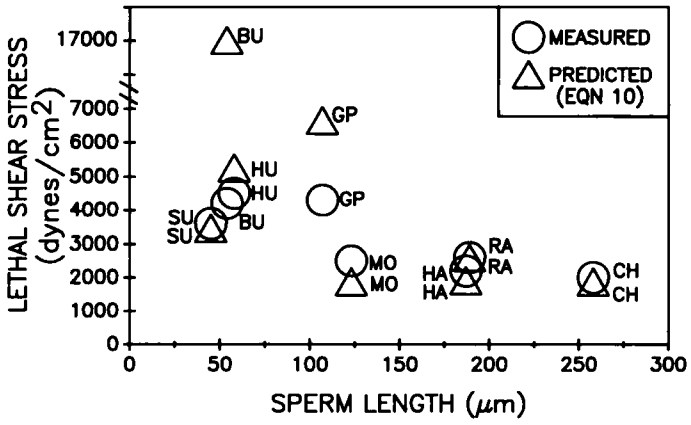

FIG. 7. Lethal shear stress as a function of the length of the sperm compared with values predicted by the model including contribution of dense fibers. The measured lethal shears are plotted vs. the length of the sperm, as in *Figure 5* (species are indicated as in Fig. 5). The measured lethal shear stresses are indicated by circles. The diamonds represent the lethal shears predicted by Equation 10 using the measured cross-sectional areas of the dense fibers. By comparing the measured value with the predicted value for each species, it can be seen that Equation 10 predicts the measured values very well. The bull sperm is an exception, with a 4-fold discrepancy between its measured lethal shear stress and the predicted value.

than would be expected from their size in the midpiece, which would lead to their being weaker than predicted. Studies such as that in human sperm by Serres et al. [13], in which the fiber geometry at known positions along the midpiece and principle piece is carefully determined, are needed for the other species if this hypothesis is to be tested.

Shear Levels in Vivo

It is important to ask whether sperm ever experience potentially lethal levels of shear stress in vivo. We can estimate the shear rate in humans during ejaculation from available data. The ejaculate traverses the vas deferens and urethra (combined length about 50 cm, width 0.05–0.12 cm [15, 16]) in about 0.1 s, yielding a velocity of approximately 500 cm/s and a shear rate of approximately 10 000 s^{-1}. To find the shear stress, we multiplied by the viscosity of the fluid. The fluids in which sperm are suspended vary greatly in their vicosities, both as a function of the location in the male tract and between species. Sperm-free bull and liquified human seminal plasmas are newtonian fluids with viscosities of 1–5 cP [17, 18]. Bull semen has a viscosity that increases with sperm concentration and is nonnewtonian in that the viscosity falls with increasing shear, from 20 cP at low shear to 5–10 cP at 200 s^{-1} [19, 18]. The fluids in which other species' sperm are suspended can be much more viscous; the apparent viscosity of rat epididymal fluid is on the order of 100 cP, and those of hamster and guinea pig are on the order of 10 cP [20]. Therefore, sperm in various mammals are suspended in fluids with viscosities ranging from 1–100 cP. Thus, the shear stresses that they suffer fall at least in the range 10^2–10^4 dynes/cm^2. Because the lethal shear stresses for most unstrengthened sperm would be a few hundred dynes/cm^2 (Fig. 5), it is clear that mammalian sperm are subjected to potentially lethal levels of shear stress in vivo, and that strengthening of the sperm

by large dense fibers appears to be necessary to insure their survival.

Is There Other Protection from Shear?

In addition to the dense fibers, large mammalian sperm may be protected from damage by other mechanisms. The sperm most in need of protection are the largest sperm which are found in the smallest animals—rodent sperm. The longest rodent sperm are stored in a highly viscoelastic mucus in the epididymis; in contrast, smaller sperm are stored in fluid that is much less viscoelastic [21, 22, 20]. It was originally thought that the immobilization of the sperm by this mucus served to depress metabolism during storage. However, it was found that rat sperm metabolism is not affected by immobilization [1]. Thus, the function of the mucus is unknown, but as proposed by Cardullo and Cone [1], it may protect sperm from shear damage. The viscosity of mucus falls dramatically when it is sheared. During flow through a tube, the mucus nearest the walls experiences the greatest shear and thus forms a low viscosity "slippage plane." The remainder of the mucus moves as a plug lubricated by this low-viscosity layer near the walls. The great majority of the sperm would be contained in the plug and would be protected from high levels of shear. The hypothesis that this functions in vivo remains to be tested.

ACKNOWLEDGMENTS

We thank Drs. David Begg and Samuel Kennedy for providing sea urchin sperm and artificial sea water and Ms. Rachel Eugster for proofreading.

REFERENCES

1. Cardullo RA, Cone RA. Mechanical immobilization of rat sperm does not change their oxygen consumption rate. Biol Reprod 1986; 34:820–830.
2. Morgenthal JC. Notes on the spermatozoal morphology of some ungulates. J S Afr Vet Med Ass 1967; 38:271–273.
3. Cummins JM, Woodall PF. On mammalian sperm dimensions. J Reprod Fert 1985; 75:153–175.
4. Baltz JM, Katz DF, Cone RA. Mechanics of sperm-egg interaction at the zona pellucida. Biophys J 1988; 54:643–654.
5. Feynmann RP, Leighton RB, Sands M. The Feynmann Lectures on Physics, vol 2. Reading, MA: Addison-Wesley Publishing Co.; 1964.
6. Jeffery GB. The motion of ellipsoidal particles immersed in a viscous fluid. Proc Roy Soc A 1923; 102:161–179.
7. Bretherton FP. The motion of rigid particles in a shear flow at low Reynolds number. J Fluid Mech 1962; 14:284–304.
8. Gray J. The movement of sea urching spermatozoa. J Exp Biol 1955; 32:775–801.
9. Rikmenspoel R. Contractile mechanisms in flagella. Biophys J 1971; 11:446–463.
10. Brokaw CJ, Gibbons IR. Mechanisms of movement in flagella and cilia. In: Wu TY-T, Brokaw CJ, Brennan C (eds.), Swimming and Flying in Nature, vol 1. New York: Plenum Press; 1975: 89–126.
11. Phillips DM. Comparative analysis of mammalian sperm motility. J Cell Biol 1972; 53:561–573.
12. Telkka A, Fawcett DW, Christensen AK. Further observations on the structure of the mammalian sperm tail. Anat Rec 1961; 141:231–245.
13. Serres C, Escalier D, David G. Ultrastructural morphometry of the human sperm flagellum with a stereological analysis of the lengths of the dense fibers. Biol Cell 1983; 49(2):153–161.
14. Fawcett DW. A comparative view of sperm ultrastructure. Biol Reprod 1970; 2(suppl):90–127.
15. Warwick R, Williams PL. Gray's Anatomy. Edinburgh: Longman; 1973: 1334.
16. Holka JF, Davis JE. Sterilization of men. In: Hafez ESE, Evans TN (eds.), Human Reproduction. Hagerstown, MD: Harper and Row; 1973: 430.
17. Dunn PF, Picologlou BF. Investigation of the rheological properties of human semen. Biorheology 1977; 14:277–292.
18. Glover FA, Scott Blair GW. The effect of sperm motility and viability on the viscosity of bull semen. Biorheology 1966; 3:189–195.
19. Mann T. The Biochemistry of Semen and the Male Reproductive Tract. London: Methuen; 1964: 86.
20. Carr DW, Usselman MC, Acott TS. Effects of pH, lactate, and viscoelastic drag on sperm motility: a species comparison. Biol Reprod 1985; 33:588–595.
21. Usselman MC, Cone RA. Rat sperm are mechanically immobilized in the caudal epididymis by "immobilin," a high molecular weight glycoprotein. Biol Reprod 1983; 29:1241–1253.
22. Usselman MC, Cone RA, Rossignol DP. Rat cauda epididymal fluid is a mucus. J Androl 1985; 6:315–320.
23. Lindemann CB, Gibbons IR. Adenosine triphosphate-induced motility and sliding of filaments in mammalian sperm extracted with triton X-100. J Cell Biol 1975; 65:147–162.
24. Yanagimachi R, Noda YD, Fujimoto M, Nicolson GL. The distribution of negative surface charges on mammalian spermatozoa. Am J Anat 1972; 135:497–520.